

Electron-impact ionization of atomic hydrogen close to threshold

N. C. Deb and D. S. F. Crothers

*Theoretical and Computational Physics Research Division, Queen's University Belfast, Belfast BT7 INN,
Northern Ireland, United Kingdom*

(Received 26 September 2001; published 8 May 2002)

A systematic study of the ionization of atomic hydrogen by electron impact from 0.3 eV to a few eV above the ionization threshold has been carried out using a semiclassical-quantal calculation. Differential and integrated cross sections are presented at 0.3 eV above the energy threshold. Triple-differential cross sections (TDCS) are presented at constant θ_{12} geometry where $\theta_{12} = 180^\circ$ and 150° . Good agreement is achieved with the measurement [Röder *et al.*, Phys. Rev. Lett. **79**, 1666 (1997)] and calculations based on exterior complex scaling at 2 eV and 4 eV above threshold. Results of triple-differential cross sections are also presented at 0.3, 0.5, and 1.0 eV above threshold at both $\theta_{12} = 180^\circ$ and 150° . At $\theta_{12} = 180^\circ$ the small local maximum in the TDCS around $\theta_1 = 90^\circ$ reported by Pan and Starace [Phys. Rev. A **45**, 4588 (1992)] at 0.5 eV above threshold is not observed in our calculation at energies down to 0.3 eV above threshold. The shape of our double differential cross sections seems to disagree qualitatively with the available calculations as we found two local maxima around 15° and 165° in our calculation. Single differential cross sections in our formulation appear naturally as a function of total excess energy E and, therefore, constant for all combinations of individual electron energies E_1 and E_2 with $E = E_1 + E_2$. Total ionization cross sections are also compared with measurement and available theoretical calculations and found to be in reasonably good agreement up to 10 eV above ionization threshold.

DOI: 10.1103/PhysRevA.65.052721

PACS number(s): 34.80.Dp, 02.60.Dc, 02.70.Bf, 31.15.-p

I. INTRODUCTION

In a plenary lecture in the recently concluded Santa Fe ICPEAC, McCurdy convincingly demonstrated why the seemingly simplest $e^- + \text{H}$ collisional process is still drawing much attention from theoreticians as well as experimentalists. This is more so because of the incomplete picture of the three-body breakup process close to the ionization threshold. In the last couple of years McCurdy and co-workers [1–7] made significant progress in the $e^- + \text{H}$ ionizing collision with their new theoretical method based on exterior complex scaling (ECS). In their formulation using an ECS transformation of the electronic coordinates they first calculate the outgoing part of the full scattering wave function over a finite volume. Then they extract the dynamical information of ionization from this scattered wave function by evaluating the quantum-mechanical flux extrapolated to an infinite volume to obtain the differential ionization cross sections. This flux-extrapolation method, however, has its limitations especially for the case of Coulomb interactions as it requires the use of large grids, to have the ionization part of the scattered wave distinguishable from the discrete two-body channels such as excitation. Further limitations are also inevitable as the excess energy $E \rightarrow 0$. To avoid these problems Baertschy *et al.* [8] presented recently a method of calculating an ionization amplitude using a “two-potential” formalism derived from the conventional distorted-wave rearrangement theory. The results presented using this method are claimed to be more accurate than those obtained by the flux-extrapolation method. This time they were able to calculate differential cross sections down to 2 eV above the threshold.

The convergent close-coupling (CCC) calculations of Bray and co-workers [9–12] have successfully produced the differential cross sections in the intermediate and high-

energy region. However, near the threshold region their results only show qualitative agreement with the corresponding measurements. Nevertheless, CCC results very close to the threshold (within 1 eV above the threshold, for example) are not yet available. The point we wish to make in this paper is that with our present semiclassical approach we can go close to the threshold (below 1-eV excess energy) without much difficulty whereas other sophisticated calculations such as ECS or CCC cannot. Beginning with the asymptotically correct [13] three-Coulomb continuum distorted-wave theory of Brauner *et al.* [14] other variants of distorted wave theories [15–20] have been reported, in studying the electron-impact ionization of hydrogen. However, as in CCC, these calculations have had reasonable success only in producing the triple differential cross sections in the intermediate and high-energy region.

Both ECS and CCC proponents presented total cross sections that are in good agreement with the measurement of Shah *et al.* [21] although their single differential cross sections exhibit qualitative differences. Scott *et al.* [22] attempted to calculate total cross section (TCS) very close to the threshold using various models within the R -matrix method and compared their TCS results only for $^1S^e$ with those predicted by various threshold laws. In a recent calculation on $e^- + \text{He}$ ionization [23] we have noted that $^1S^e$ may contribute only about 50% of the total cross sections around the threshold region. In what follows, we shall first present a brief description of our theoretical method and then present our differential (triple and double) and total cross sections followed by some concluding remarks.

II. METHOD OF CALCULATION

The uniform semiclassical wave function for the two outgoing electrons in the final channel was first obtained by

Crothers [24] by solving the corresponding Schrödinger equation in hyperspherical coordinates

$$\left[\frac{1}{\rho^5} \frac{\partial}{\partial \rho} \rho^5 \frac{\partial}{\partial \rho} + \frac{1}{\rho^2 \sin^2 2\alpha} \frac{\partial}{\partial \alpha} \sin^2 2\alpha \frac{\partial}{\partial \alpha} + \frac{4}{\rho^2 \sin \theta_{12}} \frac{\partial}{\partial \theta_{12}} \sin \theta_{12} \frac{\partial}{\partial \theta_{12}} + 2E + \frac{2\zeta(\alpha, \theta_{12})}{\rho} - \frac{2L(L+1)}{\rho^2} \right] \Psi_f^{-*} = 0, \quad (1)$$

where

$$\rho = (r_1^2 + r_2^2)^{1/2}, \quad r_1 = \rho \cos \alpha, \quad r_2 = \rho \sin \alpha,$$

$$0 \leq \rho \leq +\infty, \quad 0 \leq \alpha \leq \pi/2, \quad \cos \theta_{12} = \hat{\mathbf{r}}_1 \cdot \hat{\mathbf{r}}_2, \quad 0 \leq \theta_{12} \leq \pi,$$

and

$$\zeta = \frac{1}{\cos \alpha} + \frac{1}{\sin \alpha} - \frac{1}{(1 - \cos \theta_{12} \sin 2\alpha)^{1/2}}. \quad (2)$$

Instead of applying the JWKB ansatz to Eq. (1), Crothers [24] introduced a change in dependent variable from Ψ_f^{-*} to x , namely,

$$\Psi_f^{-*} = \frac{x |\sin(\alpha - \pi/4)|^{1/2}}{\rho^{5/2} \sin \alpha \cos \alpha (\sin \theta_{12})^{1/2}}. \quad (3)$$

Having transformed Eq. (1) accordingly he then applied the JWKB ansatz as did Peterkop [25], but to the new partial differential equation for x , namely,

$$x = P^{1/2} \exp\left(\frac{iS}{\hbar}\right). \quad (4)$$

The classical action S and density P were then obtained by solving the Hamilton-Jacobi and continuity equations, respectively. The two-electron wave function in the final channel is then given (for a detailed analysis see Ref. [26]) by

$$\begin{aligned} \Psi_f^{-*} &= \frac{c^{1/2} E^{m_{12}/2} u_1^{1/2}}{\tilde{\omega}^{1/2} \rho^{5/2} \sin \alpha \cos \alpha} \delta(\hat{\mathbf{k}}_1 - \hat{\mathbf{r}}_1) \delta(\hat{\mathbf{k}}_2 - \hat{\mathbf{r}}_2) \\ &\times \exp\left(\frac{4i}{(8Z_0\rho)^{1/2}} (\Delta\theta_{12})^{-2}\right) \exp\left[-i\left(S_0 + \frac{1}{2}\right.\right. \\ &\left.\left.\times S_1(\Delta\alpha)^2 + \frac{1}{8} S_2(\Delta\theta_{12})^2 + \frac{\pi}{4}\right) - \text{c. c.}\right], \quad (5) \end{aligned}$$

where

$$S_0 = \int_{\rho_+}^{\rho} d\tilde{\rho} \tilde{\omega}(\tilde{\rho}), \quad S_i = \rho^2 \omega(\rho) \frac{u_i'}{u_i}, \quad i = 1, 2, \quad (6)$$

$$\tilde{\omega}(\rho) = \left[\omega^2(\rho) - \omega(\rho) \left(\frac{u_2'}{u_2} - i \frac{u_i'}{u_i} \right) \right]^{1/2},$$

$$\omega^2(\rho) = 2E + 2\frac{Z_0}{\rho} - 2\frac{L(L+1)}{\rho^2}, \quad (7)$$

$$u_1 \equiv \rho^{m_{12}} {}_2F_1(m_{12}, m_{12} + 1; 2m_{12} + 3/2; -E\rho/Z_0), \quad (8)$$

$$u_2 \equiv \rho^{m_{21}} {}_2F_1(m_{21}, m_{21} + 1; 2m_{21} + 3/2; -E\rho/Z_0), \quad (9)$$

$$\rho_+ = \frac{-Z_0 + \sqrt{Z_0^2 + 4EL(L+1)}}{2E}, \quad (10)$$

$$m_{12} = -\frac{1}{4} + \frac{1}{4} \left(1 + \frac{8Z_1}{Z_0} \right)^{1/2}, \quad m_{21} = -\frac{1}{4} - \frac{1}{4} \left(1 + \frac{8Z_2}{Z_0} \right)^{1/2}, \quad (11)$$

with $Z_0 = 3/\sqrt{2}$, $Z_1 = 11/\sqrt{2}$, and $Z_2 = -1/\sqrt{2}$ and the primes in Eqs. (6) and (7) represent differentiations with respect to ρ . Notice that the classical turning point has moved to ρ_+ , the positive solution of $\omega^2(\rho) = 0$. The other solution ρ_- is classically inaccessible. The final-state wave function in Eq. (5) accounts for both radial and angular correlation through the hyperspherical coordinates. The presence of the term $\delta(\hat{\mathbf{k}}_1 - \hat{\mathbf{r}}_1) \delta(\hat{\mathbf{k}}_2 - \hat{\mathbf{r}}_2)$ in Eq. (5) is necessary to ensure that the two electrons have specific directions asymptotically and to project out the required outgoing scattering amplitude. It is also to be noted here that the classical action S in Eq. (5) has been expanded in terms of the parameters $\Delta\alpha = \alpha - \pi/4$ and $\Delta\theta_{12} = \pi - \theta_{12}$ with $\Delta\alpha = 0 = \Delta\theta_{12}$ giving the Wannier ridge angles obtained from the stationary conditions for the associated potential in Eq. (2).

The direct amplitude for the electron-impact ionization of atomic hydrogen is given by

$$f(\hat{\mathbf{k}}_1, \hat{\mathbf{k}}_2) \approx \frac{2i}{\pi} \int \Psi_f^{-*}(\mathbf{r}_1, \mathbf{r}_2) \left[\frac{1}{r_{12}} - \frac{1}{r_1} \right] e^{i\mathbf{k}_0 \cdot \mathbf{r}_1} \varphi(\mathbf{r}_2) d\mathbf{r}_1 d\mathbf{r}_2, \quad (12)$$

where $\varphi(\mathbf{r}_2)$ is the ground state of the hydrogen atom, $\Psi_f^{-*}(\mathbf{r}_1, \mathbf{r}_2)$ the final-state wave function given by Eq. (5) with momenta $\mathbf{k}_1, \mathbf{k}_2$ for the two outgoing electrons, and \mathbf{k}_0 being the momentum of the incident electron. The α integration in hyperspherical space has been evaluated by using the method of stationary phase or steepest descent, the point of stationary phase being given naturally enough by $\alpha = \pi/4$, the saddle point. The remaining integrations are done numerically using Gauss-Lobatto and Gauss-Legendre quadrature. The exchange amplitude $g(\hat{\mathbf{k}}_1, \hat{\mathbf{k}}_2)$ is obtained from the direct amplitude by interchanging θ_1 and θ_2 , the polar angles of the two outgoing electrons, with the incident beam direction as the polar axis.

The triple differential cross section (TDCS) is given by

$$\frac{d^3\sigma_I}{d\hat{\mathbf{k}}_1 d\hat{\mathbf{k}}_2 dE_1} \equiv \frac{1}{4} |f+g|^2 + \frac{3}{4} |f-g|^2. \quad (13)$$

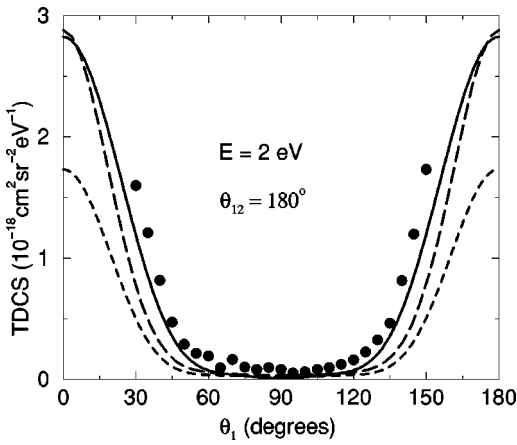


FIG. 1. Triple differential cross sections (TDCS) for single ionization of $H(1s^2S)$ by electron impact in the constant geometry of $\theta_{12}=180^\circ$ at $E=2$ eV above threshold. Filled circles, measurement [29]; dashed line, CCC results [12]; long-dashed line, ECS results [8]; and solid line, present results.

Since our final-state wave function depends on the total excess energy E and not on the individual electron energies E_1 or E_2 , the TDCS is independent of individual electron energies E_1 or E_2 . Single differential cross sections (SDCS) in our formalism will also be independent of individual electron energies E_1 or E_2 and are a function of the total excess energy E . In other words, the single differential cross section in our case is constant for any combination of E_1 and E_2 with $E=E_1+E_2$.

III. RESULTS AND DISCUSSION

Recently we have applied the above semiclassical approach to the positron impact ionization of helium [27]. During this calculation we have located an error in our subroutine for Bessel functions of large argument. That essentially means that our recently published TDCS results for electron-impact ionization of hydrogen in a Brief Report [28] need to be corrected. In this section we first present these corrected results in Figs. 1 and 2 for the $\theta_{12}=180^\circ$ geometry at 2-eV and 4-eV excess energies respectively. Recently published improved ECS results [8] and CCC [12] results and the mea-

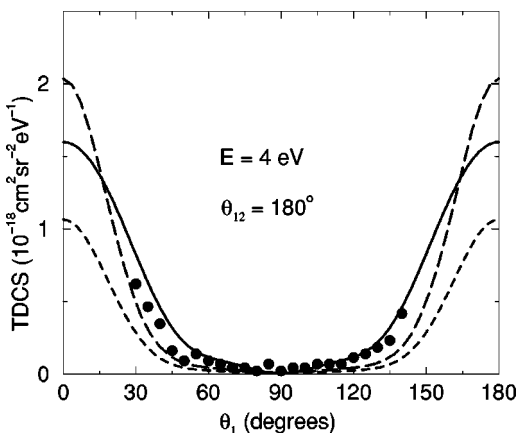


FIG. 2. Same as Fig. 1 but for $E=4$ eV.

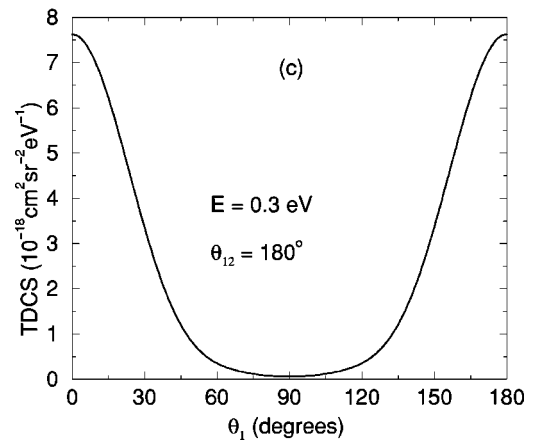
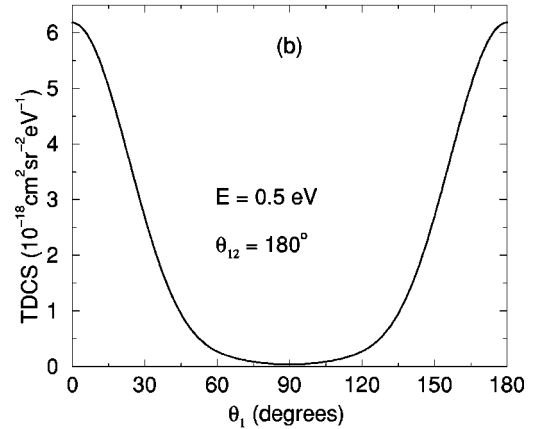
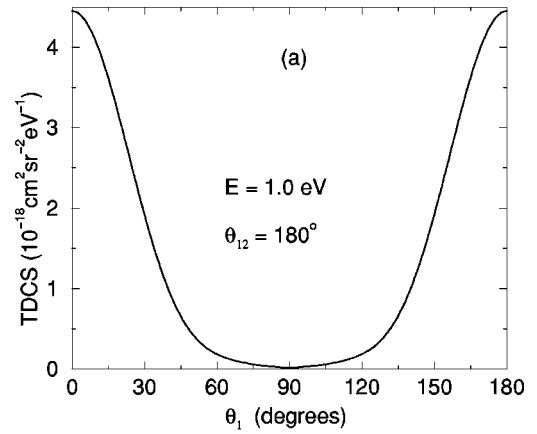


FIG. 3. Same as Figs. 1 and 2 but for (a) 1.0 eV, (b) 0.5 eV, and (c) 0.3 eV.

surements [29] are also presented in these figures for comparison. Baertschy *et al.* [8] commented that the measured TDCS at 2 eV could be too large by a factor of 2 that may have resulted from a normalization problem. They multiplied the measured values at this energy by 0.5 and compared with their results and found excellent agreement for several fixed θ_{12} angles. If this normalization problem is real then our TDCS results will be on the higher side of the measured values as is the case for 4-eV excess energy. However, the shape of our TDCS at 2 eV agrees very well with that of Baertschy *et al.* [8], over the entire angular region. At 4 eV

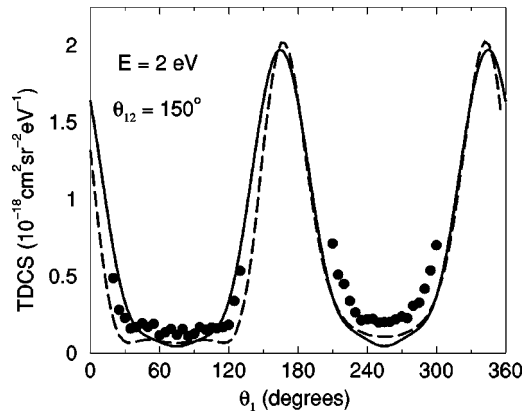


FIG. 4. TDCS for the same process as in Figs. 1–3, but in the constant geometry of $\theta_{12}=150^\circ$ at $E=2$ eV above threshold. Filled circles, measurement [30]; dashed line, ECS results [8]; and solid line, present results.

the two sets of results (present and ECS) disagree mostly at the forward and backward angles. In the absence of enough experimental points in these angular regions it is difficult to discuss the accuracy of the calculated values. In Fig. 3 we present theoretical TDCS results at 0.3-, 0.5-, and 1.0-eV excess energies above the threshold. These results show similar bowl-shaped structure. Pan and Starace [31] reported relative TDCS results at 0.5 eV calculated in their distorted partial-wave model. Their results at this energy tend to show a local maximum around $\theta_1=90^\circ$ that is not observed in our calculation, even down to 0.3-eV excess energy.

In Figs. 4 and 5 we present and compare our results for TDCS at 2- and 4-eV excess energies for $\theta_{12}=150^\circ$ geometry along with results of ECS [8] and the measurement [30]. The agreement is generally satisfactory and is better at 2 eV in terms of the cross section peaks in the entire angular region. If the experimental values at 2 eV are scaled down by a factor of two, our TDCS will slightly overestimate in the first crest region $30^\circ \leq \theta_1 \leq 120^\circ$ but will show better agreement in the second crest region $210^\circ \leq \theta_1 \leq 300^\circ$. In Figs. 6(a)–6(c) we present similar TDCS results for 1.0 eV, 0.5 eV, and 0.3 eV, respectively. These results too show the similar more strongly peaked behavior as the excess energy de-

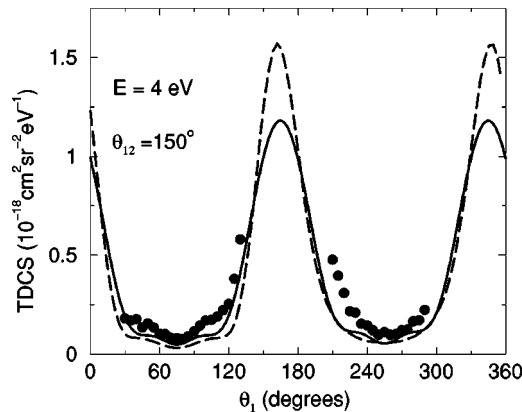


FIG. 5. Same as Fig. 4 but for $E=4$ eV.

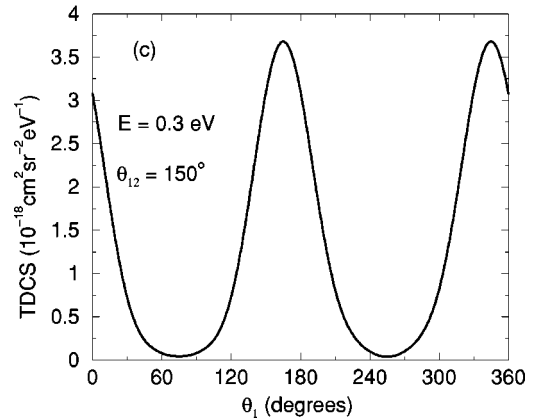
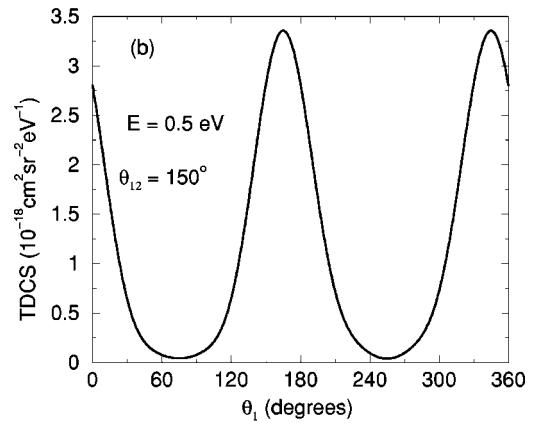
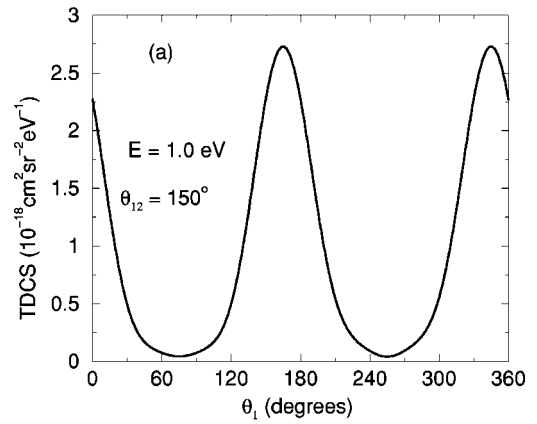


FIG. 6. Same as Figs. 4 and 5 but at (a) 1.0 eV, (b) 0.5 eV, and (c) 0.3 eV.

creases but at a slower rate than the corresponding case of $\theta_{12}=180^\circ$.

In Fig. 7 we present our double differential cross sections (DDCS) at 2 eV and 4 eV. Significant differences, both in shape and absolute value, with those of CCC results [12] are noticed. Both at forward (around 15°) and backward (around 165°) angles, our DDCS show a clear structure that is absent in the equal energy sharing results of Bray [12] and the similar ECS results [5]. In Fig. 3 of the ECS calculation of Isaacs *et al.* [5] the solid line represents the DDCS at 4-eV excess energy with $E_1=E_2=2$ eV. The numerical values of our DDCS seem to agree with those of Isaacs *et al.* [5] except at forward and backward angles whereas similar results in the

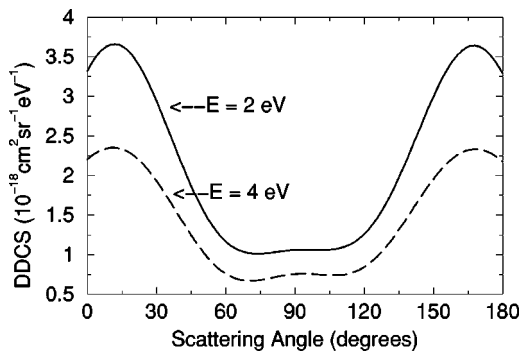


FIG. 7. Double differential cross sections (DDCS) in the present calculation. Dashed line, at 4 eV; and solid line, at 2-eV excess energies.

CCC calculation [12] appear to be lower than the present values- a trend already noticed in the TDCS results.

Figure 8 shows the comparison of our TCS with those measured by Shah *et al.* [21] and the ECS calculations by Baertschy *et al.* [7]. Close to threshold our TCS values slightly overestimate but give perfect agreement beyond 3 eV and up to 10 eV excess of threshold. Here we note that the CCC results of Bray [12] show excellent agreement with the same measurement from 2 eV up to about 100-eV excess energy. Baertschy *et al.* [7] presented TCS at only four energy points (from 17.6-eV to 30.0-eV incident electron energy) joined by the dotted line in Fig. 8, which tend also to overestimate the measurement towards the lower end of the energy scale.

In conclusion, we have presented a systematic study of electron-impact ionization of hydrogen using a quantal-semiclassical method originally developed by Crothers [24] and subsequently refined by his collaborators. The present method is relatively simple, less time consuming, and reasonably accurate in calculating the total and differential cross sections close to the ionization threshold. The final-state wave function for the outgoing particles includes proper account of the radial and angular correlations through hyperspherical coordinates. Lucey *et al.* [32] who opined that “in this very low-energy range it is perhaps asking a lot of *any*

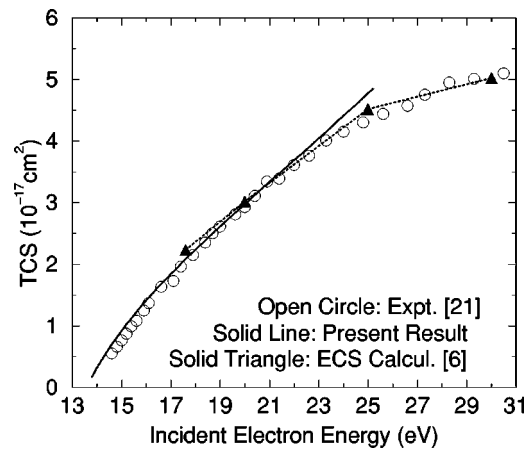


FIG. 8. Total cross sections (TCS) for the electron-impact ionization of $H(1s^2S)$ as a function of incident electron energy.

theory to reproduce experiment accurately as the three-body system is extremely correlated,” apparently overlooked the paper [24] that did predict the correct absolute size of the TCS, SDGS, DDCS, and TDCS as $E \rightarrow 0$, having predicted the correct Wannier exponent and having confirmed ergodicity. The absolute differential cross sections presented here, include, those at an energy 0.3 eV above threshold. The total cross sections are also presented and compare favorably with the measured values for the energy range 0.3 eV to 10.0 eV above threshold. Beyond this energy range our total cross sections tend to overestimate the corresponding measured values indicating that the present method based on a Wannier model may not be suitable for higher energies. Nevertheless, our method provides an extended range-of-energy validity for a Wannier type of calculation. The results very close to threshold should be tested against other calculations and measurements in the near future.

ACKNOWLEDGMENTS

This work has been supported by the Engineering and Physical Sciences Research Council (EPSRC) of the United Kingdom. We are grateful to Igor Bray and Mark Baertschy for communicating their results to us.

-
- [1] T.N. Rescigno, M. Baertschy, W.A. Isaacs, and C.W. McCurdy, *Science* **286**, 2474 (1999).
 - [2] T.N. Rescigno, C.W. McCurdy, W.A. Isaacs, and M. Baertschy, *Phys. Rev. A* **60**, 3740 (1999).
 - [3] M. Baertschy, T.N. Rescigno, W.A. Isaacs, and C.W. McCurdy, *Phys. Rev. A* **60**, R13 (1999).
 - [4] C.W. McCurdy and T.N. Rescigno, *Phys. Rev. A* **62**, 032712 (2000).
 - [5] W.A. Isaacs, M. Baertschy, C.W. McCurdy, and T.N. Rescigno, *Phys. Rev. A* **63**, 030704(R) (2001).
 - [6] C.W. McCurdy, D.A. Horner, and T.N. Rescigno, *Phys. Rev. A* **63**, 022711 (2001).
 - [7] M. Baertschy, T.N. Rescigno, W.A. Isaacs, X. Li, and C.W. McCurdy, *Phys. Rev. A* **63**, 022712 (2001).
 - [8] M. Baertschy, T.N. Rescigno, and C.W. McCurdy, *Phys. Rev. A* **64**, 022709 (2001).
 - [9] I. Bray, D.A. Konovalov, I.E. McCarthy, and A.T. Stelbovics, *Phys. Rev. A* **50**, R2818 (1994).
 - [10] I. Bray and D.V. Fursa, *Phys. Rev. Lett.* **76**, 2674 (1996); *Phys. Rev. A* **54**, 2991 (1996).
 - [11] I. Bray, *Phys. Rev. Lett.* **78**, 4721 (1997).
 - [12] I. Bray, *Aust. J. Phys.* **53**, 355 (2000); *J. Phys. B* **33**, 581 (2000).
 - [13] D.S.F. Crothers, *J. Phys. B* **15**, 2061 (1982).
 - [14] M. Brauner, J.S. Briggs, and H. Klar, *J. Phys. B* **22**, 2265 (1989).
 - [15] M. Brauner, J.S. Briggs, and J.T. Broad, *J. Phys. B* **24**, 287 (1991).

- [16] X. Zhang, C.T. Whelan, and H.R.J. Walters, *J. Phys. B* **23**, L173 (1990).
- [17] E.P. Curran, C.T. Whelan, and H.R.J. Walters, *J. Phys. B* **24**, L19 (1991).
- [18] S. Jones and D.H. Madison, *Phys. Rev. Lett.* **81**, 2886 (1998).
- [19] S. Jones and D.H. Madison, *Phys. Rev. A* **62**, 042701 (2000).
- [20] S. Jones, D.H. Madison, and D.A. Konovalov, *Phys. Rev. A* **55**, 444 (1997).
- [21] M.B. Shah, D.S. Elliot, and H.B. Gilbody, *J. Phys. B* **20**, 3501 (1987).
- [22] M.P. Scott, P.G. Burke, K. Bartschat, and I. Bray, *J. Phys. B* **30**, L309 (1997).
- [23] N.C. Deb and D.S.F. Crothers, *J. Phys. B* **34**, 143 (2001).
- [24] D.S.F. Crothers, *J. Phys. B* **19**, 463 (1986).
- [25] R.K. Peterkop, *J. Phys. B* **4**, 513 (1971).
- [26] A.M. Loughan, *Adv. Chem. Phys.* **114**, 311 (2000).
- [27] N.C. Deb and D.S.F. Crothers, *J. Phys. B* **35**, L85 (2002).
- [28] N.C. Deb and D.S.F. Crothers, *Phys. Rev. A* **64**, 034701 (2001).
- [29] J. Röder, H. Ehrhardt, C. Pan, A.F. Starace, I. Bray, and D.V. Fursa, *Phys. Rev. Lett.* **79**, 1666 (1997).
- [30] J. Röder, J. Rasch, K. Jung, C.T. Whelan, H. Ehrhardt, R.J. Allan, and H.R.J. Walters, *Phys. Rev. A* **53**, 225 (1996).
- [31] C. Pan and A.F. Starace, *Phys. Rev. Lett.* **67**, 185 (1991); *Phys. Rev. A* **45**, 4588 (1992).
- [32] S.P. Lucey, J. Rasch, and C.T. Whelan, *Proc. R. Soc. London, Ser. A* **455**, 349 (1999).